Supporting Information

Efficient Polymer Acceptor with Fluorinated Linkers Enables All Polymer Solar Cells with Efficiency of 15.7%

Haiqin Xiao,[a] Junfang Lv,[a] Miao Liu,[a] Xia Guo,[b] Xinxin Xia,[c] Xinhui Lu,[c] Maojie Zhang*[a,b]

[a]Laboratory of Advanced Optoelectronic Materials, Suzhou Key Laboratory of Novel Semiconductor-optoelectronics Materials and Devices, College of Chemistry, Chemical Engineering and Materials Science, Soochow University, Suzhou 215123, China

E-mail: mjzhang@sdu.edu.cn

[b]National Engineering Research Center for Colloidal Materials, School of Chemistry & Chemical Engineering, Shandong University, Jinan, Shandong 250100, China

[c]Department of Physics, Chinese University of Hong Kong, New Territories, Hong Kong 999077, P. R. China

1. Materials and Synthesis

All chemicals and solvents were reagent grades and purchased from Alfa Aesar, Macklin, Aldrich and TCI Chemical, respectively. Compound 1 was synthesized according to the procedure reported in the literature.[1] Compound 2 was purchased from HYRER. M2 and M3 were purchased from Solarmer. PM6 was synthesized according to the reported method.[2] The synthetic route of polymers is shown in Scheme 1 and the detailed synthesis processes are described as follows:

Synthesis of M1 (Y5-C20-Br)

Compound 1 (682 mg, 0.50 mmol) brominated 1,1-dicyanomethylene-3-indanone (**IC-Br**, 410 mg, 1.50 mmol), pyridine (950 μL), and chloroform (45 mL) were mixed in two-necked flask with argon protection. The mixture was stirred at 65 °C for 5 h. The resulted solution was poured into methanol and filtered to obtain the crude product, which was then purified using column chromatography on silica gel with dichloromethane/petroleum ether (1/2, v/v) as the eluent to give the blue-black solid **Y5-C20-Br** (769 mg, 82% yield). ^{1}H NMR (400 MHz, $CDCl_3$) ppm δ 9.18 (d, *J* = 1.7 Hz, 2H), 8.85 (d, *J* = 1.5 Hz, 1H), 8.57 (d, *J* = 8.5 Hz, 1H), 8.03 (d, *J* = 1.9 Hz, 1H), 7.87 (ddd, *J* = 8.4, 4.2, 1.7 Hz, 2H), 7.79 (dd, *J* = 7.9, 1.0 Hz, 1H), 4.76 (d, *J* = 7.7 Hz, 4H), 3.23 (t, *J* = 7.9 Hz, 4H), 2.12 (s, 2H), 1.88 (p, *J* = 7.9 Hz, 4H), 1.42 – 0.72 (m, 114H). ^{13}C NMR (100 MHz, $CDCl_3$) δ 187.3, 186.9, 159.9, 159.4, 153.6, 147.5, 145.1, 141.4, 138.5, 138.3, 137.7, 137.7, 137.2, 135.9, 135.6, 135.5, 135.5, 134.3, 134.1, 134.1, 134.1, 133.50, 133.5, 130.7, 130.1, 129.4, 128.2, 126.7, 126.4, 124.5, 120.2, 120.4, 115.2, 115.1, 114.9, 114.9, 114.5, 113.5, 113.5, 99.9, 99.7, 68.4, 68.1, 55.6, 39.1, 31.9, 31.9, 31.8, 31.8, 31.5, 30.5, 29.9, 29.8, 29.8, 29.7, 29.6, 29.6, 29.5, 29.4, 29.4, 29.4, 29.3, 29.3, 29.2, 29.2, 25.5, 22.7, 22.6, 22.6, 14.1. $C_{106}H_{136}Br_2N_8O_2S_5$ $[M^+H]^+$:1873.78. Found: 1871.99.

Synthesis of PYT

M1, (Y5-C20-Br, 80 mg, 0.0428 mmol), M2, (2,5-bis(trimethylstannyl)thiophene, 17.6 mg, 0.0428 mmol), $Pd(PPh_3)_4$ (4 mg) were combined in a 25 mL sealed tube. Dry toluene (Tol) (10 mL) was added under the argon atmosphere. The mixture was stirred

at 110 °C for 48 h. After cooled down to room temperature, the reactant mixture was poured into MeOH (50 mL). The precipitate was filtered and the obtained solid was chromatographically purified on a silica gel column eluted with chloroform to remove the impurities and oligomers. The remaining polymer was precipitated into methanol. The solid was filtered and dried under a vacuum to give the dark solid. PYT (50 mg, 50% yield).

Synthesis of PY-DF

M1, (Y5-C20-Br, 80 mg, 0.0428 mmol), M3, (2,5-bis(trimethylstannyl)thiophene, 19.1 mg, 0.0428 mmol), $Pd(PPh_3)_4$ (5.2 mg) were combined in a 25 mL sealed tube. Dry toluene (Tol) (10 mL) was added under the argon atmosphere. The mixture was stirred at 110 °C for 72 h. After cooled down to room temperature, the reactant mixture was poured into MeOH (50 mL). The precipitate was filtered and the obtained solid was chromatographically purified on a silica gel column eluted with chloroform to remove the impurities and oligomers. The remaining polymer was precipitated into methanol. The solid was filtered and dried under a vacuum to give the dark solid. PY-DF (53 mg, 51% yield).

2. Instruments and Measurements

2.1 GPC, TGA, UV-Vis-NIR absorption, CV, and PL measurements

Molecular weight of the polymers was measured by high temperature gel permeation chromatography (GPC) on an Agilent PL-GPC 220 instrument with 1,2,4 trichlorobenzene as the eluent and polystyrene as the standard at 160 °C. Thermogravimetric analysis (TGA) was obtained on a Perkin-Elmer TGA-7. UV-vis

absorption spectra were recorded on an Agilent Technologies Cary Series UV-Vis-NIR Spectrophotometer. The electrochemical cyclic voltammetry (CV) measurements were carried out on a Donghua DH7000 Electrochemical Workstation with glassy carbon disk, Pt wire, and Ag/Ag^+ electrode as working electrode, counter electrode, and reference electrode respectively, in a 0.1 M tetrabutylammonium hexafluorophosphate (Bu_4NPF_6) acetonitrile solution. Photoluminescence (PL) spectra were carried out on an Edinburgh Instrument FLS 980 spectrofluorometer.

2.2 *J-V* and EQE measurement

The current density-voltage (*J-V*) characteristics of the all-PSCs were recorded with a keithley 2450. The power conversion efficiencies were measured under 1 sun, AM 1.5G (air mass 1.5 global) (100 mW cm^{-2}) using a SS-F53A (Enli Technology CO., Ltd.) solar simulator (AAA grade, 50 mm × 50 mm photo-beam size). 2 × 2 cm^2 Monocrystalline silicon reference cell (SRC-00019, covered with a KG5 filter windows) was purchased from Enli Technology CO., Ltd. The EQE was measured by Solar Cell Spectral Response Measurement System QE-R3011 (Enli Technology CO., Ltd.). The light intensity at each wavelength was calibrated with a standard single-crystal Si photovoltaic cell.

2.3 Mobility measurement

The hole and electron mobilities were calculated by using the space-charge-limited current (SCLC) method. The corresponding charge mobilities were calculated from fitting the Mott-Gurney square law:

$$J = \frac{9\varepsilon 0\varepsilon r\mu (V\mathrm{appl} - V\mathrm{bi} - V\mathrm{s})2}{8L3}$$

Where J is the current density, ε_0 is the permittivity for free space, ε_r is the relative permittivity of the active layer (assumed to be 3), μ is the hole or electron mobility, V_{appl} is the applied voltage, V_{bi} is the built-in voltage (0 V), V_s is the voltage drop from the substrate's series resistance ($V_s = I \times R$) and L is the thickness of the active layer.

2.4 Energy loss measurement

FTPS-EQE was measured by using an integrated system (PECT-600, Enlitech), where the photocurrent was amplified and modulated by a lock-in instrument. EQE_{EL} measurement was performed by applying external voltage/current sources through the devices (ELCT-3010, Enlitech).

$$
\begin{aligned}
E_{loss} &= E_g^{PV} - qV_{oc} \\
&= \left(E_g^{PV} - qV_{oc}^{SQ}\right) + \left(qV_{oc}^{SQ} - qV_{oc}^{rad}\right) + \left(qV_{oc}^{rad} - qV_{oc}\right) \\
&= \left(E_g^{PV} - qV_{oc}^{SQ}\right) + q\Delta V_{oc}^{rad,\ below\ gap} + q\Delta V_{oc}^{non\text{-}rad} \\
&= \Delta E_1 + \Delta E_2 + \Delta E_3
\end{aligned}
$$

Where VSQ ocis the maximum voltage according to the Shockley-Queisser limit, Vrad ocis the open-circuit voltage when there is only radiative recombination.

$$
qV_{oc}^{SQ} = kT\mathrm{Ln}\left(\frac{J_{SC,SQ}}{J_{0,SQ}} + 1\right) = kT\mathrm{Ln}\left(\frac{e\int_{E_g}^{\infty} \emptyset_{AM1.5}(E)dE}{e\int_{E_g}^{\infty} \emptyset_{bb}(E)dE} + 1\right)
$$

where $\varnothing_{AM1.5}$ is the solar radiation photon flux, $\varnothing_{bb}$ is the black body radiation at 300K.

$$qV_{oc}^{rad} = kTLn\left(\frac{J_{sc}}{J_{0,rad}} + 1\right) = kTLn\left(\frac{q\int_0^{\infty} EQE\emptyset_{AM1.5}(E)dE}{q\int_0^{\infty} EQE\emptyset_{bb}(E)dE} + 1\right)$$

$$q\Delta V_{oc}^{non-rad} = -kTLn(EQE_{EL})$$

EQE_{EL} is the electroluminescence quantum efficiency.

2.5 TPC and TPV measurements

Transient photocurrent (TPC) and transient photovoltage (TPV) signals of the corresponding all-polymer solar cells were monitored using a Tektronix MDO3102 oscilloscope under a 337 nm 3.5 ns pulse laser (160 μJ per pulse at 10 Hz) and a 150 W halide lamps.

2.6 AFM and TEM measurements

Atomic force microscopy (AFM) images of blend films were recorded using a Dimension 3100 (Veeco) Atomic Force Microscope in the tapping mode. Transmission electron microscopy (TEM) was obtained by using a TePNai G2 F20 S-TWIN instrument at 200 kV accelerating voltage, in which the blend films were prepared using a processing technique, as follows: first, the blend film to be tested was spin-coated on an ITO/PEDOT:PSS substrate; then the obtained blend film on the substrate was immersed in deionized water and the separate blend film was peeled off by the interaction between PEDOT:PSS and water; finally, the blend film floating on the water surface was taken out using an unsupported 200 mesh copper mesh and used for TEM measurements.

2.7 GIWAXS measurements

GIWAXS measurements were performed at a Xeuss 2.0 SAXS/WAXS laboratory beamline using a Cu X-ray source (8.05 keV, 1.54 Å) and a Pilatus3R 300K detector with a 0.2° incidence angle. Samples were prepared on a Si substrate under the same conditions as those used for device fabrication.

2.8 Contact Angle measurement

The contact angle test was performed on a Dataphysics OCA20 Micro surface contact angle analyzer. The surface energy of the polymers was characterized and calculated by the contact angles of the two probe liquids (ultrapure water and diiodomethane) with the Owens and Wendt equation: $\gamma_{LV}(1 + \cos\theta) = 2(\gamma_S^d\gamma_L^d)^{1/2} + 2(\gamma_S^p\gamma_L^p)^{1/2}$, where γ_S and $\gamma_L$are the surface energy of the sample and the probe liquid, respectively. The superscripts d and p refer to the dispersion and polar components of the surface energy, respectively.

To calculate the wetting coefficient (ω), we should know the interfacial surface energy between different components first, which can be calculated by Neumann's equation as follows:

$$\omega_C = \frac{\gamma_{C-B} - \gamma_{C-A}}{\gamma_{A-B}}$$

where $\gamma_{X-Y}$is the interfacial surface energy between X and Y.

The interfacial surface energy can be calculated by Neumann's equation as follows:

$$\gamma_{x-y} = \gamma_x + \gamma_y - 2\sqrt{\gamma_x \cdot \gamma_y} \cdot e^{-\beta(\gamma_x - \gamma_y)^2}$$

where $\beta = 0.000115\ m^4/mJ^2$.

The location of the material C is estimated through ω_C. If $\omega_c < -1$, material C will locate in domain B. If $-1 < \omega_c < -1$, material C will locate at the interface between material A and B. If $\omega_c > 1$, material C will locate in domain A.

2.9 Device Fabrication

All devices were fabricated with a conventional device structure of ITO/PEDOT: PSS/PM6: acceptor/PFN-Br/Ag under conditions as follows: The ITO-coated glass substrates were washed three times alternately with deionized water, acetone, and isopropanol, respectively, and then sprayed dry with nitrogen gas. After surface oxygen enrichment with UV-Ozone Cleaner, PEDOT: PSS (Heraeus Clevios P VP Al 4083) was spin-coated onto the clean ITO substrate at 6000 rpm for 45 s. Subsequently, the films are annealed on a hot plate at 150 °C for 15 min. The donor and acceptor were mixed at a mass ratio of 1:1 and dissolved in chloroform (CF) at a total concentration of 16 mg/mL, and 3 wt% of 1-chloronaphthalene (CN) was added to the solution as an additive. The mixed solution was maintained at 40 °C on a hot plate and spin-coated onto the PEDOT: PSS films at 2500 rpm for 45 s, followed by annealing at 100 °C for 10 min. Then, 1 mg/mL of PFN-Br solution was spin-coated on the active layer at 2500 rpm for 30 s. At last, 100 nm Ag was vapor deposited on the films under a ca. 4×10^{-4} Pa pressure with a shadow mask to maintain the active area of the devices (0.04 cm^2).

3、Supplementary Figures. (Fig. S1-S13)

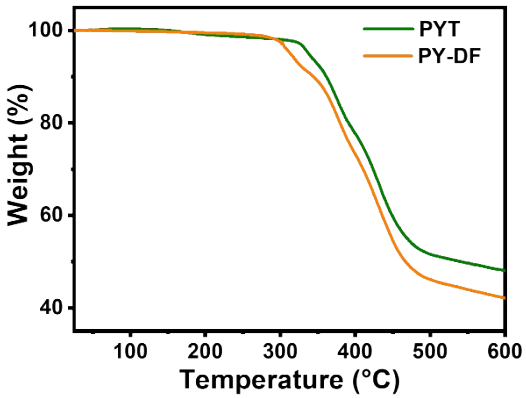

Fig. S1 TGA curves of PYT and PY-DF with a heating rate of 10 ºC min^{-1} under nitrogen atmosphere.

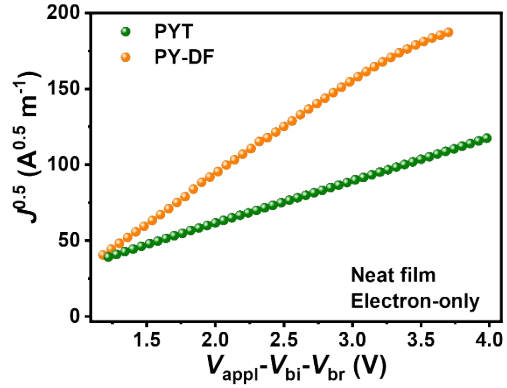

Fig. S2 The $J^{0.5}$-V plot of electron-only devices based on PYT and PY-DF neat films.

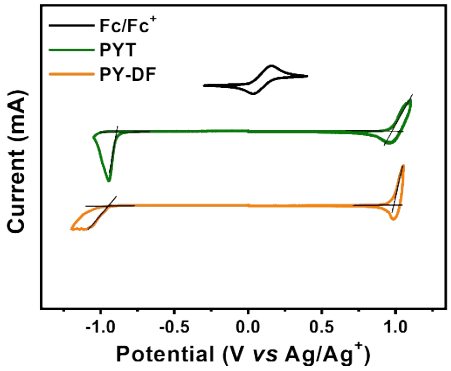

Fig. S3 Cyclic voltammograms of PYT and PY-DF films on a glassy carbon electrode measured in 0.1 mol L^{-1} Bu_4NPF_6 acetonitrile solution at a scan rate of 50 mV s^{-1}.

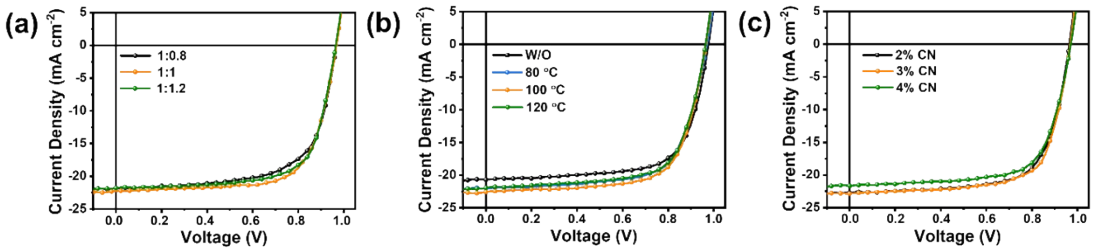

Fig. S4 The *J-V* characteristics of (a) all-PSCs based on PM6:PY-DF with different D/A weight ratios, (b) all-PSCs based on PM6:PY-DF (1:1) with different TA temperatures for 10 min and (c) all-PSCs based on PM6:PY-DF (1:1, 100 °C) with different CN content under the illumination of AM 1.5G, 100 mW cm^{-2}.

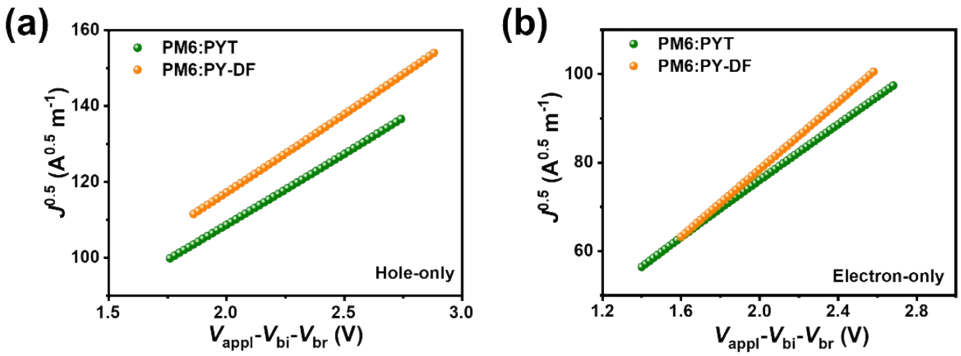

Fig. S5 The $J^{0.5}$-*V* characteristics for the corresponding (a) hole-only and (b) electron-only devices in the dark were fabricated under the optimal condition.

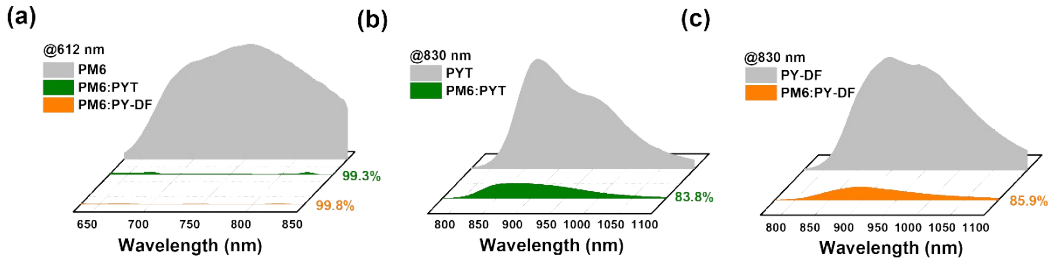

Fig. S6 (a-c) The PL spectra of PM6, PYT, PY-DF and the related blend films (excited at 612 nm for PM6, and 830 nm for PYT, PY-DF and related blend films).

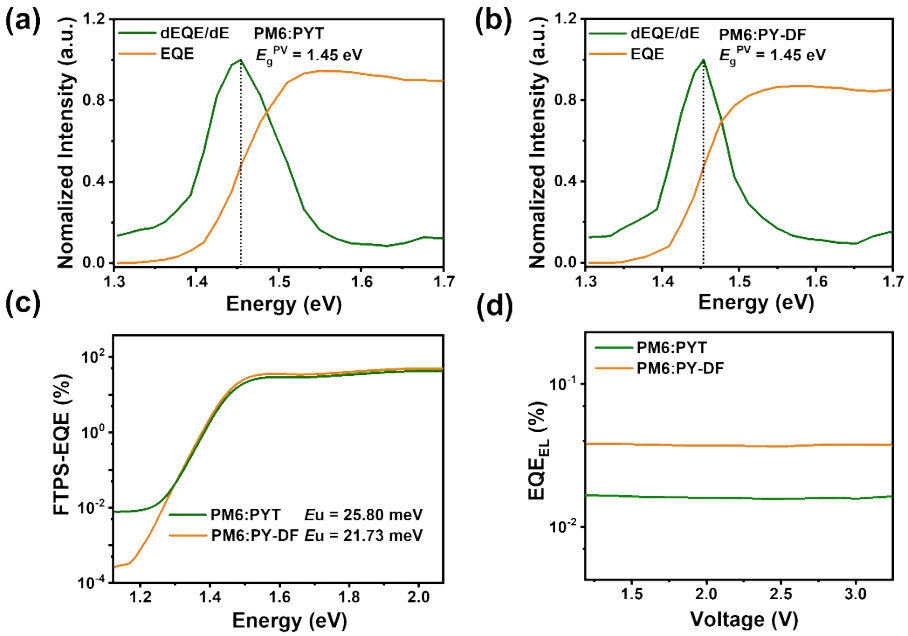

Fig. S7 (a-b) Deduction of photovoltaic bandgap from the definition of E_g^{PV}. (c) FTPS-EQE spectra and (d) EQE_{EL} curve of the PM6: PYT and PM6: PY-DF devices.

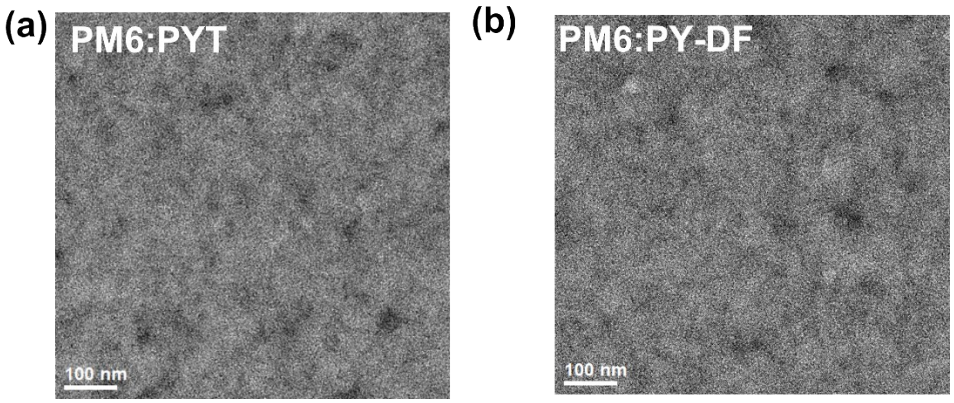

Fig. S8 TEM images of (a) PM6: PYT blend films and (b) PM6:PY-DF blend films.

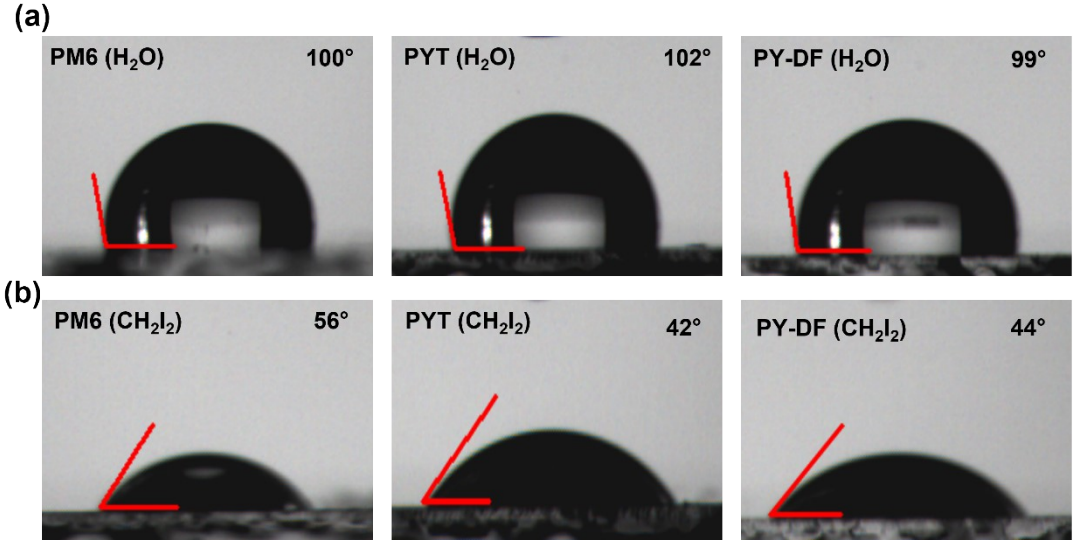

Fig. S9 Water and diiodomethane (DIM) droplet contact angles of PM6 and the PSMAs.

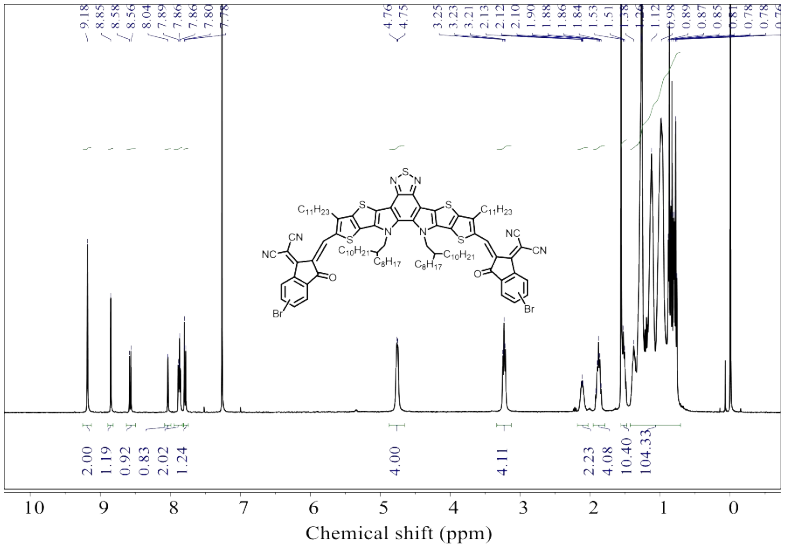

Fig. S10 ^{1}H-NMR spectrum of Y5-C20-Br (400 MHz, $CDCl_3$).

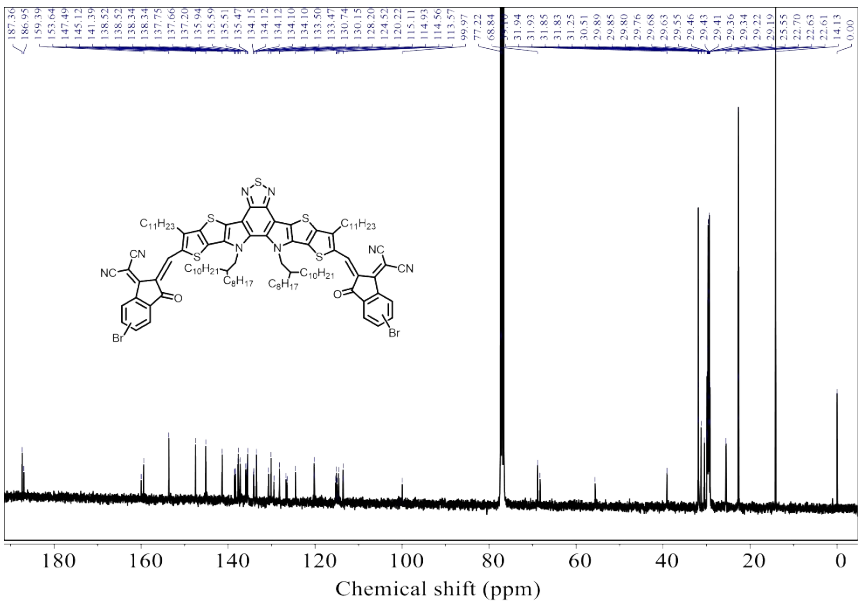

Fig. S11 ^{13}C NMR spectrum of Y5-C20-Br (100 MHz, $CDCl_3$).

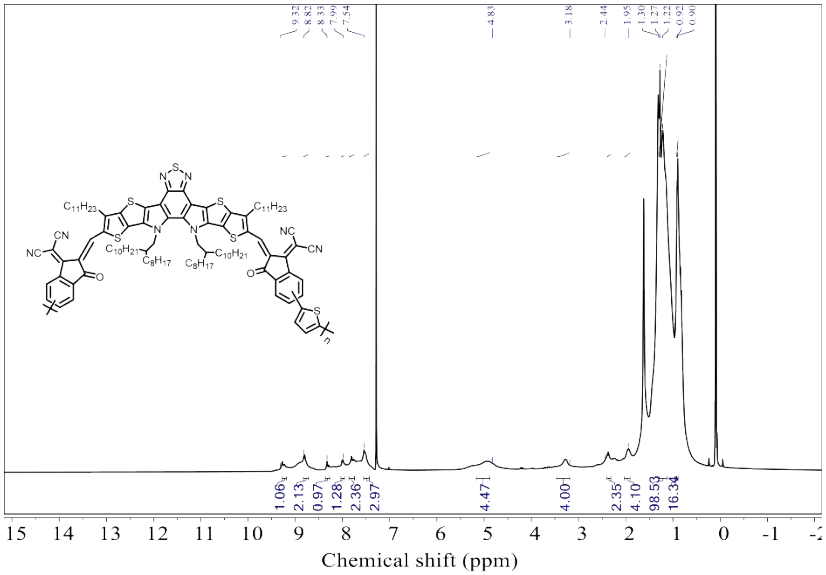

Fig. S12 ^{1}H-NMR spectrum of PYT (400 MHz, $CDCl_3$).

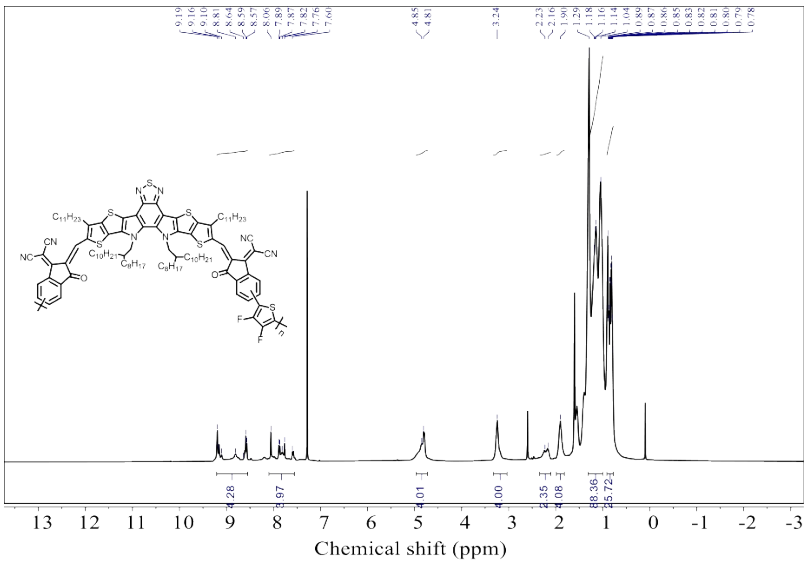

Fig. S13 ^{1}H-NMR spectrum of PY-DF (400 MHz, $CDCl_3$).

4、Supplementary Tables (Table S1-S7)

Table S1 GIWAXS parameters of the neat films of PYT and PY-DF.

Polymer	Peak		q (Å^{-1})	d (Å)	FWHM (Å^{-1})	CCL (Å)
PYT	IP	(100)	0.31	20.27	0.28	20.19
	OOP	(010)	1.63	3.85	0.35	16.15
PY-DF	IP	(100)	0.32	19.63	0.20	28.27
	OOP	(100)	0.36	17.45	0.12	47.12
		(010)	1.65	3.81	0.30	18.85

Table S2 Photovoltaic data of the all-PSCs based on PM6:PY-DF at different D/A weight ratios under the illumination of AM 1.5G, 100 mW cm^{-2}.

D/A (w/w)	V_{OC} (V)	J_{SC} (mA cm^{-2})	FF (%)	PCE (%)
1:0.8	0.97	22.0	70.1	14.8
1:1	0.97	22.4	69.8	15.1
1:1.2	0.96	21.7	69.9	14.6

Table S3 Photovoltaic data of the all-PSCs based on PM6:PY-DF (1:1) with different thermal annealing (TA) temperature for 10 min under the illumination of AM 1.5G, 100 mW cm^{-2}.

TA (°C)	V_{OC} (V)	J_{SC} (mA cm^{-2})	FF (%)	PCE (%)
W/O	0.98	20.5	69.5	13.9
80	0.97	21.9	69.0	14.6
100	0.97	22.6	69.0	15.1
120	0.96	21.9	68.7	14.5

Table S4 Photovoltaic data of the all-PSCs based on PM6:PY-DF (1:1, 100 ℃) at different CN content under the illumination of AM 1.5G, 100 mW cm^{-2}.

CN (v/v)	V_{OC} (V)	J_{SC} (mA cm^{-2})	FF (%)	PCE (%)
2	0.96	22.7	69.7	15.2
3	0.97	22.8	70.1	15.4
4	0.97	21.2	70.7	14.5

Table S5 Photovoltaic data of the representative binary all-PSCs reported previously with PCEs over 9% and this work.

Active Layer	V_{OC} (V)	J_{SC} (mA cm^{-2})	FF (%)	PCE (%)	E_{loss} (eV)	E_g^{opt} (eV)	Ref.
PBDB-T:PZ1	0.83	16.05	68.9	9.1	0.72	1.55	3
PM6:PFBDT-IDTIC	0.97	15.39	69.0	10.3	0.65	1.62	4
PM6:PF2-DTSi	0.99	16.48	66.1	10.7	0.58	1.57	5
PM6:PT-IDTTIC	0.97	17.96	67.0	11.6	0.52	1.49	6
PBDB-T:PTPBT-$ET_{0.3}$	0.90	21.33	65.3	12.5	0.52	1.41	7
PM6:PYT_M	0.93	21.78	66.3	13.4	0.52	1.42	8
PM6:L14	0.96	20.60	72.1	14.3	0.43	1.39	9
PBDB-T:PJ1	0.90	22.30	70.0	14.4	0.51	1.40	10
PM6: PYT-1S1Se	0.93	24.10	73.0	16.3	0.50	1.39	11
PM6:PYT-2Se	0.91	23.90	71.4	15.5	0.51	1.37	11
PBDB-T:PF5-Y5	0.95	20.65	74.0	14.4	0.57	1.50	12
PTzBI-oF:PFA1	0.87	23.96	72.6	15.1	0.54	141	13
PBDB-T_{MW}:PJI	0.90	22.70	75.3	15.4	—	—	14
JD40:PJ1	0.91	23.20	75.0	15.9	—	—	15

PM6:PBTIC-*γ*-2T	0.95	20.85	60.2	11.9	0.56	1.42	16
PM6:PBTIC-*γ*-2F2T	0.95	22.56	66.8	14.3	0.56	1.39	16
PM6:PY-IT	0.93	22.30	72.3	15.0	0.47	1.39	17
PM6:PY2F-T	0.86	24.27	72.6	15.2	0.52	1.37	18
PM6:L15	0.95	22.21	71.8	15.2	—	—	19
PM6:PYF-T	0.89	23.10	68.0	14.0	0.53	1.38	20
PM6:PYF-T-*o*	0.90	23.30	72.4	15.2	0.52	1.38	20
PBDB-T:PZT-*γ*	0.90	24.70	71.3	15.8	0.51	1.36	21
PM6: PY-V-*γ*	0.91	24.8	75.8	17.1	0.54	1.41	22
PM6: PY-T-*γ*	0.93	24.1	71.9	16.1	0.55	1.42	22
PM6: PY-2T-*γ*	0.93	23.5	69.9	15.3	0.56	1.43	22
PQM-Cl: PY-IT	0.92	24.3	80.7	18.0	—	—	23
PM6:PG-IT	0.96	22.8	71.4	16.1	0.54	1.47	24
PM6:PG-IT2F	0.95	23.3	75.5	17.2	0.52	1.47	24
PM6:PY-IT2F	0.91	22.2	70.0	14.1	0.54	1.45	24
PM6: PY-DF	0.97	23.1	70.2	15.7	0.48	1.45	This Work

Table S6 The contact angles and surface free energy parameters of thePM6, PYT and PY-DF neat films.

Sample	Contact angles		γ^d (mN m^{-1})	γ^p (mN m^{-1})	γ (mN m^{-1})	$(\gamma_D^{1/2} - \gamma_A^{1/2})^2$
	θ_{water}·(°)	θ_{DIM}·(°)				
PM6	100	56	30.92	0.33	31.25	—
PYT	102	42	40.80	0.02	40.82	0.64
PY-DF	99	44	38.68	0.05	38.73	0.40

Table S7 GIWAXS parameters of the blend films of PM6:PYT, and PM6:PY-DF.

Sample	Peak		q (Å^{-1})	d (Å)	FWHM (Å^{-1})	CCL (Å)
PM6:PYT	IP	(100)	0.30	20.94	0.24	23.56
	OOP	(100)	0.30	20.94	0.26	21.74
		(010)	1.66	3.78	0.26	21.74
PM6:PY-DF	IP	(100)	0.30	20.94	0.22	25.70
	OOP	(100)	0.30	20.94	0.28	20.19
		(010)	1.67	3.74	0.24	23.56

5、References

1 J. Du, K. Hu, J. Zhang, L. Meng, J. Yue, I. Angunawela, H. Yan, S. Qin, X. Kong, Z. Zhang, B. Guan, H. Ade and Y. Li, *Nat. Commun.*, 2021, **12**, 52638.

2 M. Zhang, X. Guo, W. Ma, H. Ade and J. Hou, *Adv. Mater.*, 2015, **27**, 4655-4660.

3 Z. G. Zhang, Y. Yang, J. Yao, L. Xue, S. Chen, X. Li, W. Morrison, C. Yang and Y. Li, *Angew. Chem. Int. Ed.*, 2017, **56**, 13503-13507.

4 H. Yao, F. Bai, H. Hu, L. Arunagiri, J. Zhang, Y. Chen, H. Yu, S. Chen, T. Liu, J. Y. L. Lai, Y. Zou, H. Ade and H. Yan, *ACS Energy Lett.*, 2019, **4**, 417-422.

5 Q. Fan, W. Su, S. Chen, W. Kim, X. Chen, B. Lee, T. Liu, U. A. Méndez-Romero, R. Ma, T. Yang, W. Zhuang, Y. Li, Y. Li, T.-S. Kim, L. Hou, C. Yang, H. Yan, D. Yu and E. Wang, *Joule*, 2020, **4**, 658-672.

6 H. Yao, L. K. Ma, H. Yu, J. Yu, P. C. Y. Chow, W. Xue, X. Zou, Y. Chen, J. Liang, L. Arunagiri, F. Gao, H. Sun, G. Zhang, W. Ma and H. Yan, *Adv. Energy Mater.*,

2020, **10**, 2001408.

7 J. Du, K. Hu, L. Meng, I. Angunawela, J. Zhang, S. Qin, A. Liebman-Pelaez, C. Zhu, Z. Zhang, H. Ade and Y. Li, *Angew. Chem. Int. Ed.*, 2020, **59**, 15181-15185.

8 W. Wang, Q. Wu, R. Sun, J. Guo, Y. Wu, M. Shi, W. Yang, H. Li and J. Min, *Joule*, 2020, **4**, 1070-1086.

9 H. Sun, H. Yu, Y. Shi, J. Yu, Z. Peng, X. Zhang, B. Liu, J. Wang, R. Singh, J. Lee, Y. Li, Z. Wei, Q. Liao, Z. Kan, L. Ye, H. Yan, F. Gao and X. Guo, *Adv. Mater.*, 2020, **32**, 2004183.

10 T. Jia, J. Zhang, W. Zhong, Y. Liang, K. Zhang, S. Dong, L. Ying, F. Liu, X. Wang, F. Huang and Y. Cao, *Nano Energy*, 2020, **72**, 104718.

11 Huiting Fu, Qunping Fan, Wei Gao, Jiyeon Oh, Yuxiang Li, Francis Lin, Feng Qi, Changduk Yang, Tobin J. Marks and A. K.-Y. Jen, *Sci. China. Chem.*, 2022, **65**, 309-317.

12 Q. Fan, Q. An, Y. Lin, Y. Xia, Q. Li, M. Zhang, W. Su, W. Peng, C. Zhang, F. Liu, L. Hou, W. Zhu, D. Yu, M. Xiao, E. Moons, F. Zhang, T. D. Anthopoulos, O. Inganäs and E. Wang, *Energy Environ. Sci.*, 2020, **13**, 5017-5027.

13 F. Peng, K. An, W. Zhong, Z. Li, L. Ying, N. Li, Z. Huang, C. Zhu, B. Fan, F. Huang and Y. Cao, *ACS Energy Lett.*, 2020, **5**, 3702-3707.

14 L. Zhang, T. Jia, L. Pan, B. Wu, Z. Wang, K. Gao, F. Liu, C. Duan, F. Huang and Y. Cao, *Sci. China. Chem.*, 2021, **64**, 408-412.

15 B. Lu, Z. Zhang, J. Wang, G. Cai, J. Wang, X. Yuan, Y. Ding, Y. Wang and Y. Yao, *Mater. Chem. Front.*, 2021, **5**, 5549-5572.

16 H. Wang, H. Chen, W. Xie, H. Lai, T. Zhao, Y. Zhu, L. Chen, C. Ke, N. Zheng and F. He, *Adv. Funct. Mater.*, 2021, **31**, 2100877.

17 Z. Luo, T. Liu, R. Ma, Y. Xiao, L. Zhan, G. Zhang, H. Sun, F. Ni, G. Chai, J. Wang, C. Zhong, Y. Zou, X. Guo, X. Lu, H. Chen, H. Yan and C. Yang, *Adv. Mater.*, 2020, **32**, 2005942.

18 H. Yu, S. Luo, R. Sun, I. Angunawela, Z. Qi, Z. Peng, W. Zhou, H. Han, R. Wei, M. Pan, A. M. H. Cheung, D. Zhao, J. Zhang, H. Ade, J. Min and H. Yan, *Adv. Funct. Mater.*, 2021, **31**, 2100791.

19 H. Sun, B. Liu, Y. Ma, J. W. Lee, J. Yang, J. Wang, Y. Li, B. Li, K. Feng, Y. Shi, B. Zhang, D. Han, H. Meng, L. Niu, B. J. Kim, Q. Zheng and X. Guo, *Adv. Mater.*, 2021, **33**, 2102635.

20 H. Yu, M. Pan, R. Sun, I. Agunawela, J. Zhang, Y. Li, Z. Qi, H. Han, X. Zou, W. Zhou, S. Chen, J. Y. L. Lai, S. Luo, Z. Luo, D. Zhao, X. Lu, H. Ade, F. Huang, J. Min and H. Yan, *Angew. Chem. Int. Ed.*, 2021, **60**, 10137-10146.

21 H. Fu, Y. Li, J. Yu, Z. Wu, Q. Fan, F. Lin, H. Y. Woo, F. Gao, Z. Zhu and A. K. Jen, *J. Am. Chem. Soc.*, 2021, **143**, 2665-2670.

22 H. Yu, Y. Wang, H. K. Kim, X. Wu, Y. Li, Z. Yao, M. Pan, X. Zou, J. Zhang, S. Chen, D. Zhao, F. Huang, X. Lu, Z. Zhu and H. Yan, *Adv. Mater.*, 2022, **34**, 2200361.

23 J. Wang, Y. Cui, Y. Xu, K. Xian, P. Bi, Z. Chen, K. Zhou, L. Ma, T. Zhang, Y. Yang, Y. Zu, H. Yao, X. Hao, L. Ye and J. Hou, *Adv. Mater.*, 2022, **34**, 2205009.

24 G. Sun, X. Jiang, X. Li, L. Meng, J. Zhang, S. Qin, X. Kong, J. Li, J. Xin, W. Ma

and Y. Li, *Nat. Commun.*, 2022, **13**, 5267.